

## Research Article

# Effects of Soybean Oil Modified Cellulose Fibril and Organosilane Modified Cellulose Fibril on Crystallization of Polypropylene

Sarit Thanomchat<sup>1</sup> and Kawee Srikulkit<sup>1,2</sup>

<sup>1</sup>Department of Materials Science, Faculty of Science, Chulalongkorn University, Bangkok 10330, Thailand

<sup>2</sup>Center of Excellence on Petrochemical and Materials Technology, Chulalongkorn University, Bangkok 10330, Thailand

Correspondence should be addressed to Kawee Srikulkit; [kawee@sc.chula.ac.th](mailto:kawee@sc.chula.ac.th)

Received 29 September 2015; Accepted 2 December 2015

Academic Editor: Wenbin Yi

Copyright © 2015 S. Thanomchat and K. Srikulkit. This is an open access article distributed under the Creative Commons Attribution License, which permits unrestricted use, distribution, and reproduction in any medium, provided the original work is properly cited.

Soybean oil modified cellulose fibril (Oil-g-CF) and organosilane modified cellulose fibril (Silane-g-CF) were prepared using maleinized soybean oil and hexadecyltrimethoxysilane, respectively. Thus obtained modified cellulose fibril was added to polypropylene by a simple melt mixing on a hotplate. PP/modified CF composites with 4.0 wt% filler content were prepared. The composites were subject to a polarized optical microscope to investigate particle dispersion, supramolecular morphology, and crystallization behavior. It was found that Silane-g-CF exhibited smaller particle sizes with better particle distribution when compared to Oil-g-CF. In addition, the etched composite samples unveiled an increase in a number of spherulite crystals as well as a decrease in the spherulite size. The nonisothermal crystallization study of composites revealed that both Oil-g-CF and Silane-g-CF were capable of nucleating PP by facilitating faster crystallization process and raising the number of spherulites. The DSC results indicated that Silane-g-CF was able to perform a more effective nucleation than Oil-g-CF, judged by a higher crystallization temperature. Moreover, PP composites containing Oil-g-CF and Silane-g-CF had higher crystallinity by 7% and 10%, for the first and the latter, respectively, when compared to neat PP.

## 1. Introduction

Polymer composites which consist of a polymer matrix and a reinforcing filler belong to materials having improved properties including high strength and stiffness, good impact resistance, and light weight [1, 2]. Well-known applications of composite materials include fiberglass tanks and carbon fiber reinforced products (aerospace, automotive, and sport goods). In recent years, an interest in cellulose reinforcing materials has been continuously increasing due to their attractive properties such as high strength and stiffness, low density, biodegradability, and renewability [3, 4]. Cellulose belongs to polysaccharides which consist of 3,000 or more glucose units. It is the most abundant of all naturally occurring polymers [5]. Also, it is of great economic importance. The chemical structure of cellulose is a linear homopolysaccharide of  $\beta$ -1,4-linked anhydro-D-glucose units and the

repeating unit is called anhydroglucose unit or AGU [6]. Cellulose can be prepared in a variety of forms including film, fiber, microcrystalline cellulose, and nanocellulose.

Nanocellulose, having at least one dimension in nanometers range [5], can be classified into two types including cellulose nanocrystal and cellulose fibril. Cellulose nanocrystal (CNC), also called rod-like colloidal particle, nanocrystalline cellulose, cellulose whisker, or cellulose microcrystallite, has a rod-like shape of 5–70 nm in width and 100 nm to few micrometers in length. CNC is a nearly completely crystalline cellulose obtained by hydrolysis of cellulose fiber using a mineral acid under controlled condition. The amorphous region becomes soluble under hydrolysis reaction, leaving perfect crystalline cellulose particle [6–8]. On the contrary, cellulose fibril (CF) known as cellulose microfibril, microfibrillar cellulose, or nanocellulose is extracted by mechanical treatments of cellulosic fibers such as homogenization,

microfluidization, grinding, and cryocrushing without the acid hydrolysis. CF consists of both amorphous and crystalline parts and exhibits a web-like structure with the diameter ranging from 20 to 60 nm and the length is several micrometers [6–9]. Usually, CF is widely used as thickening agent, emulsifier, or additive in foods, paints, coatings, cosmetics, and pharmaceutical industries [3]. The interesting properties of CF including high aspect ratio, high strength and stiffness, good barrier property, and light weight are attractive for the application as a reinforcement in nanocomposites by enhancing modulus, tensile strength, barrier property, and crystallization temperature [4, 10, 11]. However, CF direct addition to hydrophobic polymers such as polyethylene (PE), polypropylene (PP), poly(lactic acid) (PLA), or polycaprolactone (PCL) results in its poor dispersibility in polymer matrix due to the hydrophilicity of cellulose. Moreover, CF itself when left drying freely presents in hard aggregate form, making the dispersion of the hard aggregate impossible. Therefore, the surface modification of CF by chemical treatments including silanization, acetylation, and grafting is required to improve the dispersibility as well as compatibility with polymer matrix [5, 12, 13].

In this work, CF obtained by the dissolution/precipitation technique of microcrystalline cellulose (MCC) [14] was modified by two different types of modifying agents including maleinized soybean oil and hexadecyltrimethoxysilane. Thus obtained modified CF was employed as a filler for PP matrix. Simple mixing on a hotplate was carried out. After that, PP composite was characterized to investigate the effect of those two types of fillers on the crystallization behavior of polypropylene.

## 2. Materials and Methods

**2.1. Materials.** Cellulose fibril (CF) was prepared according to the previous report [14]. Soybean oil was kindly provided by Siam Chemical Industry, Co., Ltd., Thailand. Maleic anhydride (Fluka) and dicumyl peroxide 98% (Aldrich Chemistry) were of analytical grade. Hexadecyltrimethoxysilane (Dynasylan 9116) was kindly supplied by Evonik. Nonylphenol ethoxylate EO15 (EO15) under the trade name of TERGITOL by DOW Chemical Company was kindly provided by local supplier (StarTechChemical Co., Ltd.). Polypropylene chip (HP561R, HMC Polymers, Thailand) was ground into powder prior to use.

**2.2. Synthesis of Soybean Oil Modified Cellulose Fibril (Oil-g-CF).** Maleinized soybean oil was synthesized by the reaction of soybean oil with maleic anhydride in the presence of dicumyl peroxide as an initiator. Firstly, a 500 mL Erlenmeyer flask containing soybean oil (100 g) and 20 g of maleic anhydride (20 wt% of soybean oil) were prepared. Then, dicumyl peroxide (1 g, 5 wt% based on maleic anhydride) was added. The mixture was stirred and heated to 170°C and kept at this temperature for 3 h. After that, the viscous yellowish liquid was left standing at ambient temperature overnight to allow the precipitation of unreacted maleic anhydride. The 40 g of viscous yellowish liquid was decanted to another container where 200 g (10 g on dry weight) of

acetone extracted cellulose fibril gel was present. 200 mL of dry acetone was added to reduce the mixture viscosity. The CF/maleinized soybean oil mixture was stirred for 2 h and cured at 120°C for 3 h in an oven. Excessive maleinized soybean oil was washed off by acetone, resulting in soybean oil modified cellulose fibril (Oil-g-CF) which was ground to powder and passed through a 140 mesh sieve screen. The tentative structure of Oil-g-CF is represented in Scheme 1.

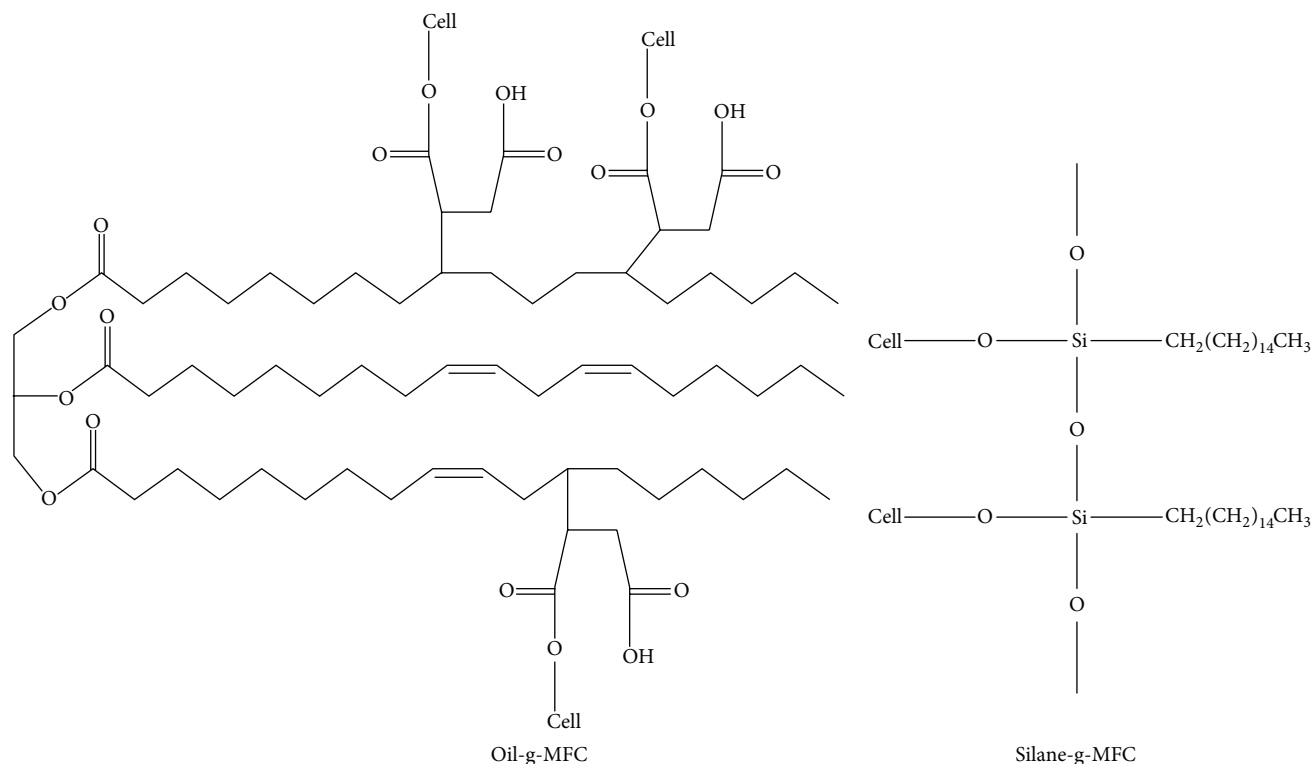
**2.3. Synthesis of Organosilane Modified Cellulose Fibril (Silane-g-CF).** 200 g of wet CF (equivalent to 10 g of dry CF) was dispersed into 200 mL of 10% v/v EO15. Then, 25 g of hexadecyltrimethoxysilane (2.5:1.0 HDTMS:CF wt ratio) was added to the CF dispersion and followed by 5 g of methanol (3-fold by mole of cellulose). Then, glacial acetic acid was added drop by drop until pH value reached pH 2-3. After vigorous stirring for 3 h, the mixture was put in an oven with the temperature set at 60°C to accelerate silanization reaction for 1 h. The resultant Silane-g-CF was washed off, dried, and then ground. Grinded powder was sieved through a 140-mesh sieve screen. The tentative structure of Silane-g-CF is also represented in Scheme 1.

**2.4. Simple Preparations of PP/Oil-g-CF and PP/Silane-g-CF Composites.** The PP/CF composites were made by a simple melt mixing on a hotplate. Cellulose fibril powder to PP weight ratio of 1:24 was chosen. Firstly, the PP powder was physically mixed with modified CF powder and then sandwiched between polyimide films. The composite was heated to 210°C on a hot plate for 2 minutes. The molten PP was flattened, resulting in a thin film, and then removed from the hotplate. The film was repeatedly folded, molten, and flattened for 4 cycles to obtain a PP/CF composite film with a thickness of  $25.0 \pm 5 \mu\text{m}$ .

**2.5. Characterizations.** FTIR analysis (transmission mode) of KBr disk sample was performed using a spectrometer (Nicolet 6700, Thermo Electron Corporation). IR spectrum was recorded between  $4,000 \text{ cm}^{-1}$  and  $400 \text{ cm}^{-1}$ . The morphology of Oil-g-CF and Silane-g-CF was observed by a scanning electron microscope (JSM 6460 LV, Jeol, Japan). The particle size distribution of modified CF was measured by dynamic light scattering technique using a particle size analyzer (Brookhaven Instruments Corp., USA). The dispersion of modified CF in PP was studied using a polarized optical microscope (CX31, Olympus, Japan) under a transmittance light. The composite film was prepared on a glass slide and covered with a cover slip before characterization.

To study the crystalline morphology, all films were chemically etched in an etching solution containing 1% of potassium permanganate in a solution of 10:4:1 (v/v) 98% sulphuric acid, 85% orthophosphoric acid, and water to remove amorphous region [15]. The crystalline morphology including size and number was observed by a scanning electron microscope (JSM 6460 LV, Jeol, Japan).

The nonisothermal crystallization behavior of PP and composites were investigated using the polarized optical microscope (DMR, Leica, Germany) equipped with a hot stage (METTLER TOLEDO, USA) under a cross-polarized



SCHEME 1: Chemical structures of Oil-g-CF and Silane-g-CF.

and digital camera. The film sample was placed between a glass slide and a cover slip on the hot stage. The composite film was observed using a polarized microscope. The sample was heated from 30°C to 210°C with a heating rate of 20°C min<sup>-1</sup> and held at 210°C for 5 min to remove the thermal history. Then, the sample was cooled to 30°C with a cooling rate 10°C min<sup>-1</sup> and the crystallization behavior was recorded every 10 seconds by a digital camera.

The thermal stability of CF, modified CF, neat PP, and composites was characterized by TGA (TGA/STDA851, METTLER TOLEDO, USA). About 5.0 mg of sample was heated from 50 to 600°C under nitrogen atmosphere at a flow rate of 20 mL min<sup>-1</sup>.

The thermal properties of neat PP and composites were investigated by DSC (DSC1, METTLER TOLEDO, USA). The 1.0–2.0 mg of sample was measured within temperature range of 0–220°C under nitrogen atmosphere at a flow rate of 50 mL min<sup>-1</sup>. The heating rate was 10°C min<sup>-1</sup>. To eliminate the thermal history of polymer, the specimen was held at 220°C for 3 min. Then, the specimen was cooled down from 220°C to 0°C at cooling rate of 10°C min<sup>-1</sup>. This procedure was repeated twice.

### 3. Results and Discussion

**3.1. FTIR Analysis of Oil-g-CF and Silane-g-CF.** Figure 1 shows the FT-IR spectra of CF, Oil-g-CF, and Silane-g-CF. The CF spectrum shows the characteristic absorption bands of typical cellulose. The O-H stretching presents broadly

between 3200 and 3600 cm<sup>-1</sup> and the C-H stretching band shows up at 2871 cm<sup>-1</sup>. The absorption band at 1640 cm<sup>-1</sup> is attributable to the characteristic IR absorption band of bound water, indicating the extremely high water content present in CF network. The absorption vibrations at 1153 cm<sup>-1</sup>, 1041 cm<sup>-1</sup>, and 899 cm<sup>-1</sup> correspond to the C-O stretching of cellulose, the vibration of C-O-C pyranose ring skeleton, and the characteristic of β-glucosidic linkages of glucose units, respectively [16]. Referring to the spectrum of Oil-g-CF, the disappearance of O-H band at 3400 cm<sup>-1</sup> indicates the successful hydrophobicity modification of CF. The two absorption bands at 2911 cm<sup>-1</sup> and 2846 cm<sup>-1</sup> correspond to the symmetric and asymmetric stretching vibration of CH<sub>2</sub> groups, respectively. The band at 1750 cm<sup>-1</sup> is attributed to the carbonyl vibration arising from maleinized soybean oil [17]. Spectrum of Silane-g-CF exhibits the strong absorption bands at 2911 cm<sup>-1</sup> and 2846 cm<sup>-1</sup> responsible for the symmetric and asymmetric vibrations of silane CH<sub>2</sub> moieties. Absorption bands between 3100 cm<sup>-1</sup> and 3500 cm<sup>-1</sup> and at 1650 cm<sup>-1</sup> are attributable to the silica silanol (Si-OH) group, indicating the presence of partially free silanol groups. The rocking and symmetric stretching of SiO<sub>2</sub> intertetrahedral oxygen atoms showed up at 450 cm<sup>-1</sup> and 800 cm<sup>-1</sup>, respectively. The symmetric stretching of SiO<sub>2</sub> intertetrahedral oxygen atoms at 1080 cm<sup>-1</sup> and the absorption band of Si-O-C between 1000 cm<sup>-1</sup> and 1150 cm<sup>-1</sup> are found overlapped with the primary and secondary alcohol groups of cellulose [18].

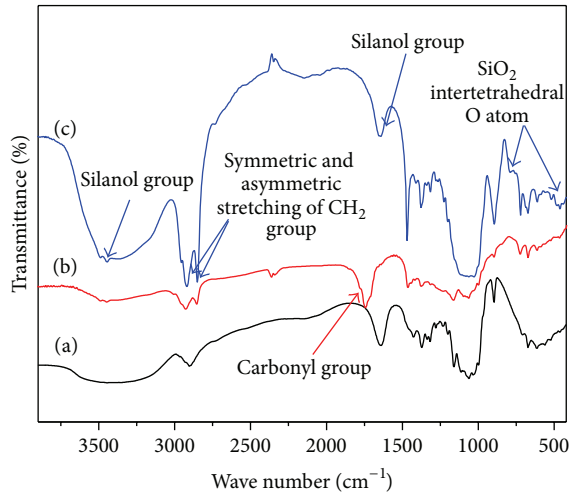


FIGURE 1: FTIR spectra of (a) CF, (b) Oil-g-CF, and (c) Silane-g-CF.

**3.2. Morphology.** The morphology was investigated by SEM as shown in Figure 2. From SEM analysis, CF is present in gel-like form. In fact, when observed by high resolution equipment (FE-SEM), CF was found in a form of nanofibril web [14]. The morphological images of Oil-g-CF and Silane-g-CF are found totally different from the virgin CF. As seen, Oil-g-CF presents in large agglomerate due to the characteristic of surface hydrophobicity. In a similar manner, the morphology of Silane-g-CF is also observed in the form of agglomerate particles. Interestingly, modified CF particles exhibited soft agglomeration which was proven by their high swellability in nonpolar solvents (toluene). Hence, it was expected that modified CF particles would easily be dispersed in plastics including polypropylene particularly when extrusion mixing is employed. On the other hand, virgin CF stayed intact in toluene, indicating the hard aggregation characteristic.

**3.3. Particle Size Distribution.** The particle size distributions of CF, Oil-g-CF, and Silane-g-CF are shown in Figure 3. Deionized water was employed as a medium for CF due to its hydrophilic characteristic. On the other hand, toluene was employed as a medium for Oil-g-CF and Silane-g-CF. The result shows a broad range of particle size distributions with an average diameter of 560 nm in case of CF, whereas the average diameters of Oil-g-CF and Silane-g-CF are 1700 nm and 850 nm, respectively. An increase in size of modified CF particles is indicative of soft agglomeration characteristic due to the fact that modified CF particles exhibited swellability in nonpolar solvent.

**3.4. Dispersion Study of Oil-g-CF and Silane-g-CF in PP.** The optical micrographs of neat PP (Figure 4(a)) and PP/4 wt% Oil-g-CF composite (Figure 4(b)) and PP/4 wt% Silane-g-CF (Figure 4(c)) are presented. Neat PP film is clearly transparent under the optical microscope. For PP/Oil-g-CF composite, particles are found scattered and present in agglomerate with the particle sizes ranging from 70  $\mu\text{m}$  up to 200  $\mu\text{m}$  which is significantly larger than the original size measured by the

particle size analyzer. The larger agglomerates of Oil-g-CF indicate that cohesive force among particles is stronger than adhesion force between Oil-g-CF and PP. In a similar manner, Silane-g-CF particle sizes in range between 40 and 80  $\mu\text{m}$  are observed in case of PP/Silane-g-CF composite. Change in CF particle size reflects that modified CF exhibits meltability characteristic which plays a key role in wetting plastics, consequently resulting in filler particles with compatibility as well as dispersibility.

**3.5. Crystalline Morphology.** The remaining crystalline morphology of etched specimens after removal of amorphous region by chemical etching is illustrated in Figure 5. The spherulite crystal is obviously seen in all cases. However, the number of spherulites in composite samples seems to be not different from those of neat PP. In a similar manner, the spherulite diameters are almost the same in all cases. It may be a result of smaller spherulite removal by chemical etching. Optical microscopic observation under hot stage is employed to confirm that modified CF plays a nucleation role in accelerating the crystallization process, leading to smaller spherulite sizes due to the nucleation density [19, 20].

**3.6. Nonisothermal Crystallization Behavior.** The crystallization behavior of neat PP and composites is presented in Figure 6. In case of neat PP, the spherulites are observed at 120°C. For composites, nucleation begins at 125°C evidenced by the presence of small spherulites which grow up continuously when the temperature is gradually cooled down. When compared to neat PP at 120°C, both composites show faster growth rate judged by the spherulite size and a number of spherulites. The crystallization process of PP/Silane-g-CF and PP/Oil-g-CF composite is complete at 115°C while neat PP still continues to crystallize. These results indicate that both types of modified CF are able to act as a nucleating agent for PP due to its faster crystallization performance. The nucleation ability of both particles was associated with a number of tiny particle sizes of fillers with large surface area which facilitated nucleation sites for spherulite growth. In contrast, neat PP contained the absence of nucleating site, resulting in slower nucleation process.

**3.7. Thermal Stability.** The TG thermograms in Figure 7 reveal the thermal stability of CF, modified CF, neat PP, and composites. In Figure 7(a), all types of cellulosic materials show a small weight loss around 60–100°C corresponding to the evaporation of water [18]. The loss of water is prominent in case of CF gel due to its hydrophilic characteristic. CF begins to degrade at 270°C ( $T_{\text{onset}}$ ) which is significantly lower than those of modified CF. The relatively low degradation temperature of CF is associated with the moisture present, accelerating the thermal degradation of cellulose by hydrolysis reaction. In comparison to unmodified CF, the  $T_{\text{onset}}$  of Oil-g-CF is at 325°C, indicating the higher thermal stability due to the lack of bound moisture. In another case, Silane-g-CF exhibits two degradation steps at 300°C and at 450°C. The second degradation step corresponds to the decomposition of grafted silane [21, 22]. The effect of modified CF on the thermal stability of neat PP is shown in Figure 7(b). The

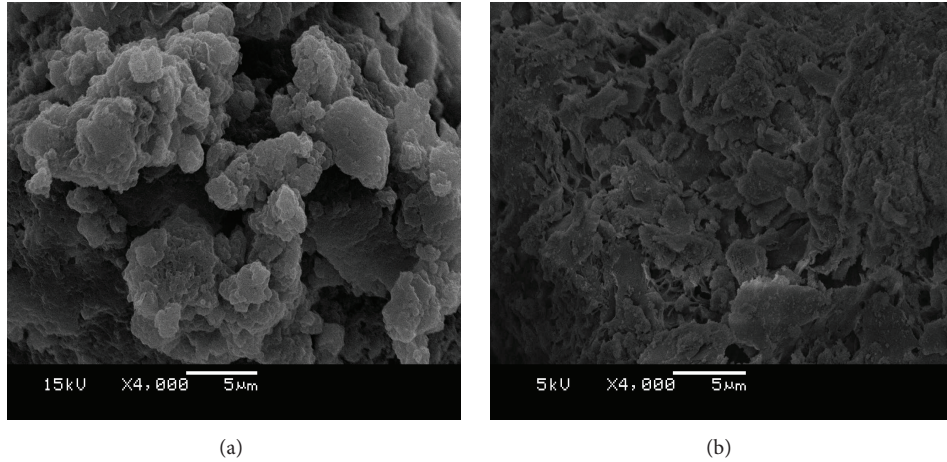


FIGURE 2: SEM images of (a) Oil-g-CF and (b) Silane-g-CF.

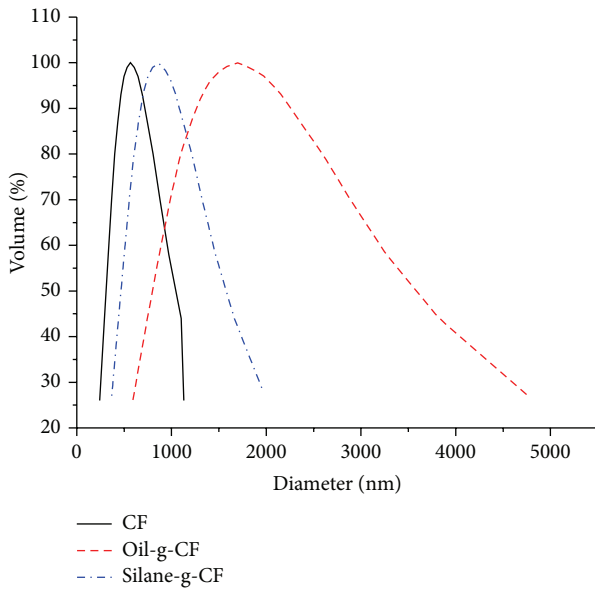


FIGURE 3: Particles size distributions of CF, Oil-g-CF, and Silane-g-CF by dynamic light scattering.

results indicate that the addition of Oil-g-CF and Silane-g-CF can enhance the thermal stability of PP evidenced by the degradation temperature of PP composites shifting up by 20°C when compared to neat PP.

**3.8. Thermal Properties.** As seen in Figure 8(a) and Table 1, DSC heating curves of all samples show only a single melting peak of  $\alpha$ -form crystals [23, 24]. The melting peak ( $T_m$ ) of neat PP is found at 155°C whereas both composites exhibit higher melting temperatures, indicating that modified CF could improve thermal properties of PP. However, the addition of Oil-g-CF just slightly raises the melting temperature by 1°C whereas the prominent higher melting temperature can be observed in case of Silane-g-CF filled PP with the increase of melting temperature up to 161°C. As shown in

TABLE 1: Thermal properties of neat PP and PP/Oil-g-CF composite and PP/Silane-g-CF composite at the second heating and cooling scan.

Sample	$T_m$ (°C)	$\Delta H_m$ (J/g)	$X_c$ (%)	$T_c$ (°C)	$\Delta H_c$ (J/g)
Neat PP	155.4	69.9	33.4	114.7	73.7
PP/Oil-g-CF	156.4	81.3	40.5	115.0	86.2
PP/Silane-g-CF	161.3	89.1	44.4	118.6	91.9

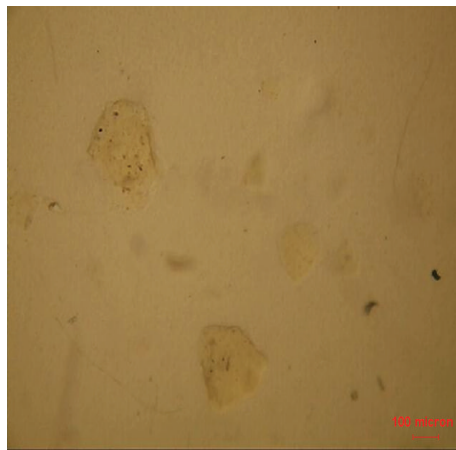
Table 1, the rising melting temperature corresponds to an increase in percent crystallinity. The addition of Oil-g-CF and Silane-g-CF results in an increase in percent crystallinity ( $X_c$ ) of PP up to 7 and 10%, respectively. The cooling exotherm shown in Figure 8(b) demonstrates better nucleation performance of Silane-g-CF than Oil-g-CF judged by higher crystallization temperature ( $T_c$ ) of PP approximately 4°C. In comparison with Silane-g-CF, the nucleation ability of Oil-g-CF is leveled off by the plasticization effect of Oil-g-CF.

## 4. Conclusions

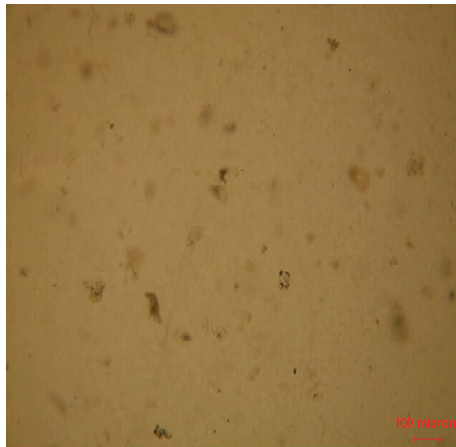
Cellulose fibril (CF) from dissolution/precipitation technique was modified by two different types of modifying agents including maleinized soybean oil and hexadecyltrimethoxysilane, resulting in Oil-g-CF and Silane-g-CF, respectively. Nucleation performances between Oil-g-CF and Silane-g-CF on polypropylene were compared. Based on  $T_c$  values, Silane-g-CF was more capable of nucleating PP than Oil-g-CF, arising from its smaller particle sizes. The addition of Silane-g-CF and Oil-g-CF was found to enhance the thermal stability of PP by raising the degradation temperatures of PP up by 20°C in both cases. The study of crystal morphology and crystallization behavior showed that modified CF accelerated PP crystallization, obtaining the faster crystallization process which produced the higher number of spherulites and smaller spherulite sizes when compared to neat PP. The melting temperature and percent



(a)

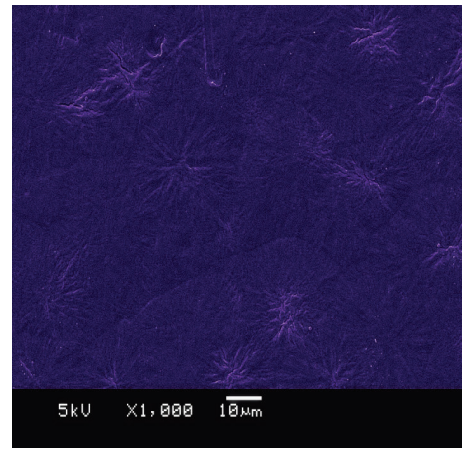


(b)

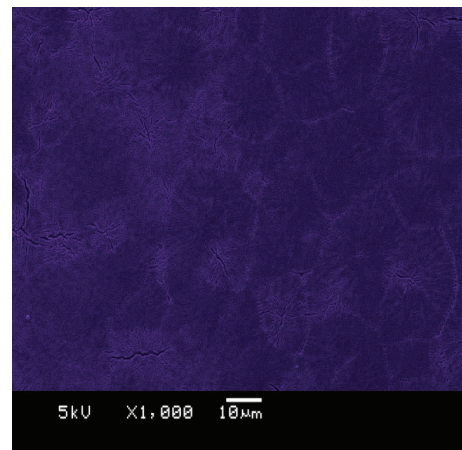


(c)

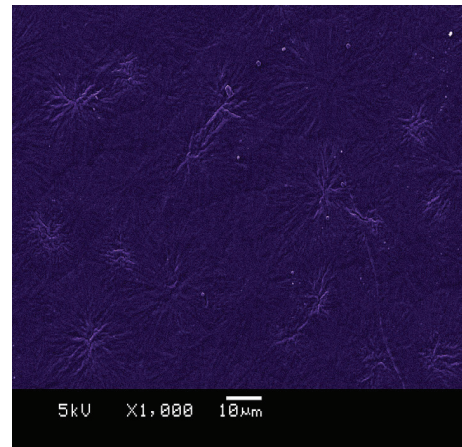
FIGURE 4: Optical micrographs (transmission mode) of (a) neat PP, (b) PP/Oil-g-CF composite, and (c) PP/Silane-g-CF composite with 4.0 wt% filler loading (scale bar 100  $\mu\text{m}$ ).



(a)



(b)



(c)

FIGURE 5: SEM images of etched film (a) neat PP, (b) PP/Oil-g-CF composite, and (c) PP/Silane-g-CF composite at 4.0 wt% filler loading (scale bar 10  $\mu\text{m}$ ).

crystallinity were also found to be higher in case of composites. In addition, the prominent nucleating effect was observed in Silane-g-CF filled PP composite due to the

smaller particles size while Oil-g-CF failed to play an effective nucleation role due to the interference of Oil-g-CF in terms of plasticization effect. It is expected that the CF/PP composite

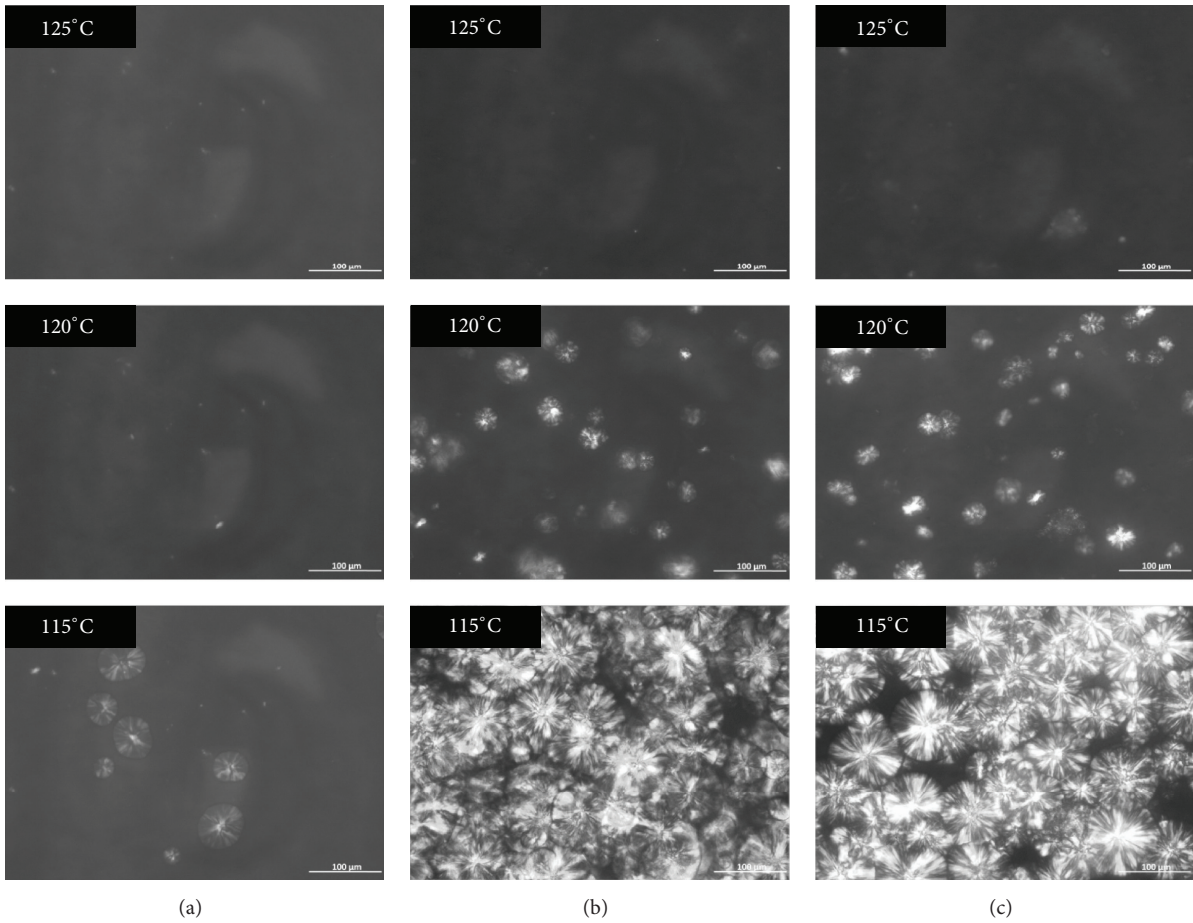


FIGURE 6: Optical micrographs of crystallization process of (a) neat PP, (b) PP/Oil-g-CF composite, and (c) PP/Silane-g-CF composite (scale bar 100 μm).

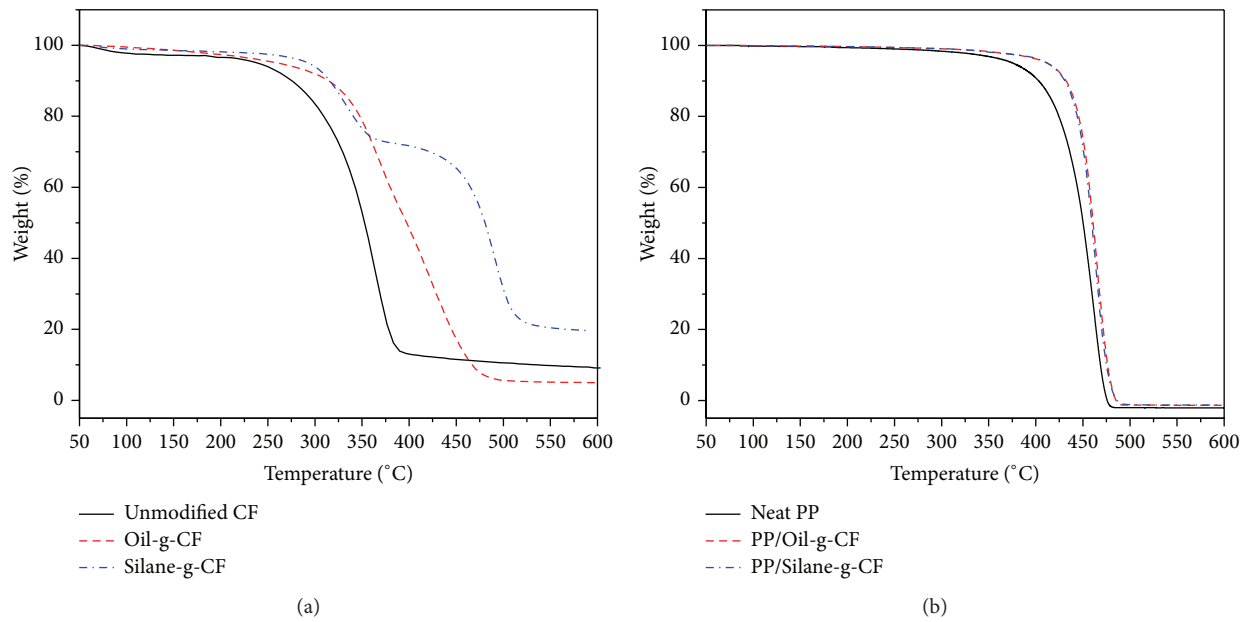


FIGURE 7: TG thermograms of (a) CF, Oil-g-CF, and Silane-g-CF and (b) neat PP, PP/Oil-g-CF, and PP/Silane-g-CF.

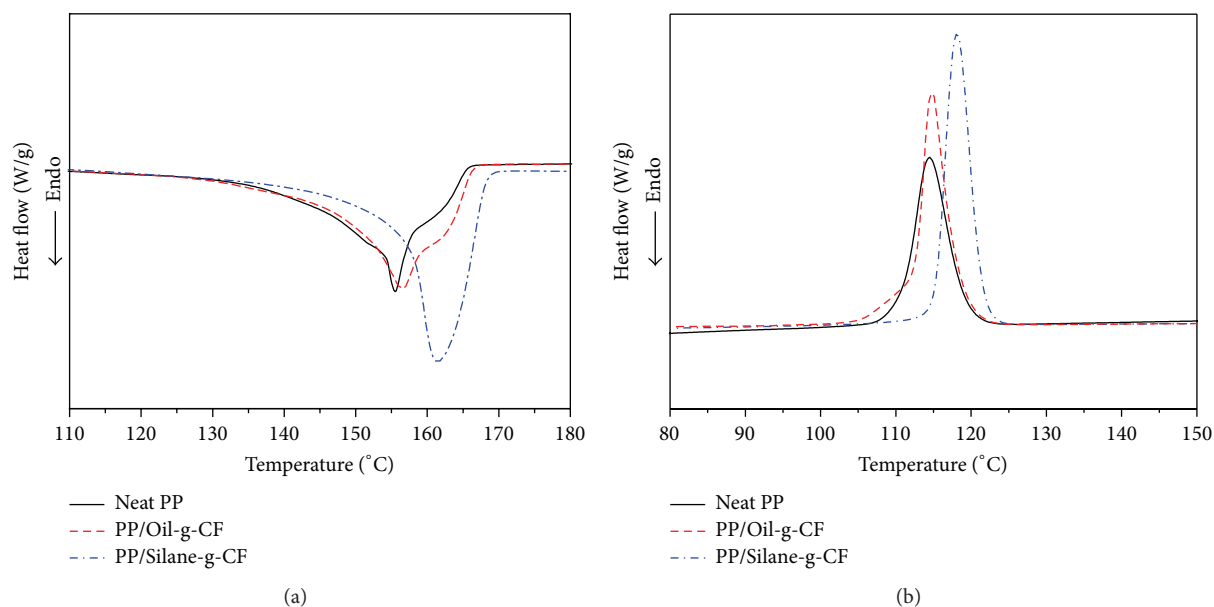


FIGURE 8: DSC thermograms of neat PP, PP/Oil-g-CF composite, and PP/Silane-g-CF composite: (a) second heating curves and (b) second cooling curves.

would exhibit an improvement in mechanical properties as well as thermal properties due to the nucleation effect as well as reinforcement characteristic of cellulose fibril.

### Conflict of Interests

The authors declare no conflict of interests.

### Acknowledgments

The authors would like to thank The 90th Anniversary of Chulalongkorn University (Ratchadaphiseksomphot Endowment Fund GCUGR1125582011D) and the Royal Golden Jubilee Ph.D. Program (PHD/0182/2553) for the support of this work.

### References

- [1] J. Lu, P. Askeland, and L. T. Drzal, "Surface modification of microfibrillated cellulose for epoxy composite applications," *Polymer*, vol. 49, no. 5, pp. 1285–1296, 2008.
- [2] J. P. Jose, S. K. Malhotra, S. Thomas, K. Joseph, K. Goda, and M. S. Sreekala, *Polymer Composites: Volume 1*, Wiley-VCH, 1st edition, 2012.
- [3] K. L. Spence, R. A. Venditti, Y. Habibi, O. J. Rojas, and J. J. Pawlak, "The effect of chemical composition on microfibrillar cellulose films from wood pulps: mechanical processing and physical properties," *Bioresource Technology*, vol. 101, no. 15, pp. 5961–5968, 2010.
- [4] J. Lu, T. Wang, and L. T. Drzal, "Preparation and properties of microfibrillated cellulose polyvinyl alcohol composite materials," *Composites Part A: Applied Science and Manufacturing*, vol. 39, no. 5, pp. 738–746, 2008.
- [5] H. P. S. Abdul Khalil, Y. Davoudpour, M. N. Islam et al., "Production and modification of nanofibrillated cellulose using various mechanical processes: a review," *Carbohydrate Polymers*, vol. 99, pp. 649–665, 2014.
- [6] N. Lavoine, I. Desloges, A. Dufresne, and J. Bras, "Microfibrillated cellulose—its barrier properties and applications in cellulosic materials: a review," *Carbohydrate Polymers*, vol. 90, no. 2, pp. 735–764, 2012.
- [7] A. Carlmark, E. Larsson, and E. Malmström, "Grafting of cellulose by ring-opening polymerisation—a review," *European Polymer Journal*, vol. 48, no. 10, pp. 1646–1659, 2012.
- [8] X. Xu, F. Liu, L. Jiang, J. Y. Zhu, D. Haagensohn, and D. P. Wiesenborn, "Cellulose nanocrystals vs. Cellulose nanofibrils: a comparative study on their microstructures and effects as polymer reinforcing agents," *ACS Applied Materials and Interfaces*, vol. 5, no. 8, pp. 2999–3009, 2013.
- [9] I. Siró and D. Plackett, "Microfibrillated cellulose and new nanocomposite materials: a review," *Cellulose*, vol. 17, no. 3, pp. 459–494, 2010.
- [10] S. Iwamoto, S. Yamamoto, S.-H. Lee, and T. Endo, "Mechanical properties of polypropylene composites reinforced by surface-coated microfibrillated cellulose," *Composites Part A: Applied Science and Manufacturing*, vol. 59, pp. 26–29, 2014.
- [11] A. N. Nakagaito, A. Fujimura, T. Sakai, Y. Hama, and H. Yano, "Production of microfibrillated cellulose (MFC)-reinforced polylactic acid (PLA) nanocomposites from sheets obtained by a papermaking-like process," *Composites Science and Technology*, vol. 69, no. 7-8, pp. 1293–1297, 2009.
- [12] S. Kalia, S. Boufi, A. Celli, and S. Kango, "Nanofibrillated cellulose: surface modification and potential applications," *Colloid and Polymer Science*, vol. 292, no. 1, pp. 5–31, 2014.
- [13] H. P. S. Abdul Khalil, A. H. Bhat, and A. F. Ireana Yusra, "Green composites from sustainable cellulose nanofibril: a review," *Carbohydrate Polymers*, vol. 87, no. 2, pp. 963–979, 2012.
- [14] S. Thanomchat, K. Srikulkit, B. Suksut, and A. K. Schlarb, "Morphology and crystallization of polypropylene/cellulose fibril composites," *KMUTNB International Journal Applied Science and Technology*, vol. 7, no. 4, pp. 23–34, 2014.



- [15] M. Wang, L. Lin, Q. Peng, W. Ou, and H. Li, "Crystallization and mechanical properties of isotactic polypropylene/calcium carbonate nanocomposites with a stratified distribution of calcium carbonate," *Journal of Applied Polymer Science*, vol. 131, no. 10, pp. 1–9, 2014.
- [16] W. Y. Li, A. X. Jin, C. F. Liu, R. C. Sun, A. P. Zhang, and J. F. Kennedy, "Homogeneous modification of cellulose with succinic anhydride in ionic liquid using 4-dimethylaminopyridine as a catalyst," *Carbohydrate Polymers*, vol. 78, no. 3, pp. 389–395, 2009.
- [17] S. Spoljaric, A. Genovese, and R. A. Shanks, "Polypropylene—microcrystalline cellulose composites with enhanced compatibility and properties," *Composites Part A: Applied Science and Manufacturing*, vol. 40, no. 6-7, pp. 791–799, 2009.
- [18] S. Sequeira, D. V. Evtuguin, I. Portugal, and A. P. Esculcas, "Synthesis and characterisation of cellulose/silica hybrids obtained by heteropoly acid catalysed sol–gel process," *Materials Science and Engineering C*, vol. 27, no. 1, pp. 172–179, 2007.
- [19] A. K. Schlarb, D. N. Suwitaningsih, M. Kopnarski, and G. Niedner-Schatteburg, "Supermolecular morphology of polypropylene filled with nanosized silica," *Journal of Applied Polymer Science*, vol. 131, no. 1, Article ID 39655, pp. 1–8, 2013.
- [20] Y. He and Y. Inoue, "Effect of  $\alpha$ -cyclodextrin on the crystallization of poly(3-hydroxybutyrate)," *Journal of Polymer Science Part B: Polymer Physics*, vol. 42, no. 18, pp. 3461–3469, 2004.
- [21] A. Rachini, M. Le Troedec, C. Peyratout, and A. Smith, "Comparison of the thermal degradation of natural, alkali-treated and silane-treated hemp fibers under air and an inert atmosphere," *Journal of Applied Polymer Science*, vol. 112, no. 1, pp. 226–234, 2009.
- [22] W. Shen, H. He, J. Zhu, P. Yuan, and R. L. Frost, "Grafting of montmorillonite with different functional silanes via two different reaction systems," *Journal of Colloid and Interface Science*, vol. 313, no. 1, pp. 268–273, 2007.
- [23] J. Dai, Y. Shen, J.-H. Yang, T. Huang, N. Zhang, and Y. Wang, "Crystallization and melting behaviors of polypropylene admixed by graphene and  $\beta$ -phase nucleating agent," *Colloid and Polymer Science*, vol. 292, no. 4, pp. 923–933, 2014.
- [24] J. Duan and Q. Dou, "Investigation on  $\beta$ -polypropylene/PP-g-MAH/surface treated talc composites," *Journal of Applied Polymer Science*, vol. 130, no. 1, pp. 206–221, 2013.



# Hindawi

Submit your manuscripts at  
<http://www.hindawi.com>

